International Journal of Engineering Technology Science and Research
IJETSR
www.ijetsr.com
ISSN 2394 – 3386
Volume 4, Issue 9
September 2017

Raman Microscopy and Electron Beam Analysis in Characterisation of an Iron Smelting Slag from Tumu Hills, Manipur, India

Md Raheijuddin Sheikh
Director DDU KAUSHAL Kendra
Dhanamanjuri Community College,
D M College of Science, Imphal Manipur, India

Abstract:
A sample of iron slag from the traditional iron making site at TumuChing, Manipur, India about 60 kilometres south from the capital city of Manipur, was characterised by various physical techniques. In this paper, the results of characterisation by using Raman microscopy (RM) and electron beam analysis (EBA) have been presented. The phases identified in a slag found at an iron making site not only reflect the chemical composition of the slag but can also provide crucial information regarding the reconstruction and interpretation of the metallurgical operations, such as the prevailing redox conditions in a furnace at the time of cooling. Free iron oxides, such as haematite, magnetite and wustite, are important indicators of these redox conditions. By combining the results provided by RM and EBA, it was possible to identify the free iron oxides, haematite and magnetite in the original ore, and magnetite and wustite in the slag.

1. Introduction

Characterization of iron and its slag obtained from various parts of India has been well documented [1-3]. The chronology of early Iron Age smelting technologies is also documented [4, 5]. The Dhatwa iron was found to be produced through small crucible type furnace where limonite type ore was reduced. The slag obtained from such sites was found to be fayalite (SiO_3Fe) [6-8]. The slag obtained from a small hill called TumuChing in Manipur has been characterized by X-ray fluorescence, X-ray diffraction, Fourier transform infrared spectroscopy, optical microscopy and the dating of the slag was carried out using thermo luminescence dating technique [9-11].

Iron oxide is the dominant component in almost all ancient copper and iron smelting slags, typically averaging from 50 to 70 wt% in the bulk composition. Most of this is present as iron silicate, typically as crystalline fayalite (Fe_2SiO_4) or in a glass of near fayalitic composition, also containing oxides not compatible with the fayalite structure such as alumina, lime and potash. In systems high in alumina, hercynite ($FeAl_2O_4$) or a solid solution between hercynite and magnetite (Fe_3O_4) forms. If the iron oxide in the melt system exceeds the amount necessary to combine all silica and alumina in one or other of these phases, any surplus iron oxides crystallises as one of the various iron oxides, namely haematite (α-Fe_2O_3), magnetite or wustite(FeO), depending on the redox conditions prevailing at the time of cooling and crystallisation. These free iron oxides, as distinct from the iron oxide chemically bonded in silicate phases, are therefore important indicators of the redox conditions prevailing in the furnace or hearth at the time of slag solidification, providing potentially critical information for process reconstruction and interpretation.

Under equilibrium conditions, the redox conditions should express themselves as a specific ratio of iron in its two common oxidation states, constant across the entire sample from a specific smelt. However, few ancient furnaces achieved full equilibrium conditions. Disequilibrium can be due to incomplete reactions following premature termination of the process and subsequent freezing of the status quo in the crystallising slag, but also regularly reflects local gradients in oxygen supply in the furnace.

International Journal of Engineering Technology Science and Research
IJETSR
www.ijetsr.com
ISSN 2394 – 3386
Volume 4, Issue 9
September 2017

Fig.1. APhoto of the iron smelting site at TumuChing, Manipur (Source: Author)

Further complications arise from post-process alterations, beginning with tapping, and including the slow oxidation during burial over extended periods, often under humid conditions. As a result, ancient metallurgical slag often exhibits over the distance of a few millimetres a range of redox conditions, from strongly reducing iron-forming to more oxidising, resulting in the decomposition of fayalite into magnetite and silica at high temperature or the formation of ferricfayalite at ambient conditions. In the extreme, the conditions would include fully oxidised areas with prevalent haematite (formed hot) or any of the iron hydroxides due to weathering. Quantifying the exact oxidation state of iron in slag is therefore an important means of reconstructing process parameters as well as post-process alterations, and there are several established methods for this. However, both classical rapid oxidation during removal of liquid slag from the furnace titration of a solution and Mossbauer spectroscopy of a prepared powder rely on the analysis of relatively large amounts of material to provide a bulk average oxidation state, and cannot distinguish between primary redox conditions and later digenetic changes following burial. The quantitative analysis of oxidation gradients within a given sample and the identification of post-process alterations both require a spatially resolved, image-based method of oxidation state determination. A basic identification of these is routinely achieved using reflected light microscopy, distinguishing the various free iron oxides by their specific optical properties and morphologies, and also enabling the rapid identification of post process alterations such as re-deposition of iron hydroxide in cracks and voids, and the partial oxidation of fayalite. However, both magnetite and wustite can form non-stoichiometric crystals, and the correct identification of the oxidation state within either of these is necessary for a more detailed process reconstruction. It is suggested that Raman microscopy (RM) is a useful method to quantify the oxidation state of the iron.

2.1. Electron beam analysis

Phase identification was supported by a JEOL 8600 Superprobe electronmicroscope using 20 kV accelerating voltage and a beam current of 80 nA. The instrument was calibrated with pure elements or simple binary compounds, and analytical totals were in the range 98–102 wt%. Spectra were collected using an energy-dispersive detector with INCA software. Raw elemental intensities relative to the pure standard intensities were corrected using a ZAF procedure to adjust for atomic number, absorption and fluorescence effects, calculating the oxygen by stoichiometry assuming all iron to be present as Fe_2^+.

2.2. Raman microscopy

Raman microscopy (RM) was carried out using a Renishaw 1000 spectrometer, equipped with a Renishaw He–Ne laser operating at 632.8 nm at a power of 0.35 mW. The system was calibrated to better than 1 cm−1 using a neon lamp before measurement. The different crystals in the slag sample werelocated using a Leica microscope incorporated into the Renishawsystem. Analyses were performed on small particle aggregates, a procedure preferentially used for dark materials, due to the strong coupling between dark materials and the laser light.Spectra were recorded as an extended scan.

International Journal of Engineering Technology Science and Research
IJETSR
www.ijetsr.com
ISSN 2394 – 3386
Volume 4, Issue 9
September 2017

3. Results and Discussion:

Optical microscopy (OM) observation of the slag sample allowed a distinction to be made between different regions according to the different stages of formation and subsequent crystallization of the slag. The different regions in the iron slag have been considered in the following figures

Fig.2. a piece of lumpy iron slag collected from the area. The black shiny matrix is the physical characteristics that indicate the presence of silica; the reddish colour shows the probability of some iron contents. The big bubbles indicates that air has been blown to fire the ore minerals in the process of iron smelting and the air and water vapour trapped after the iron was extracted leaves these bubbles and vacuoles in the slag.

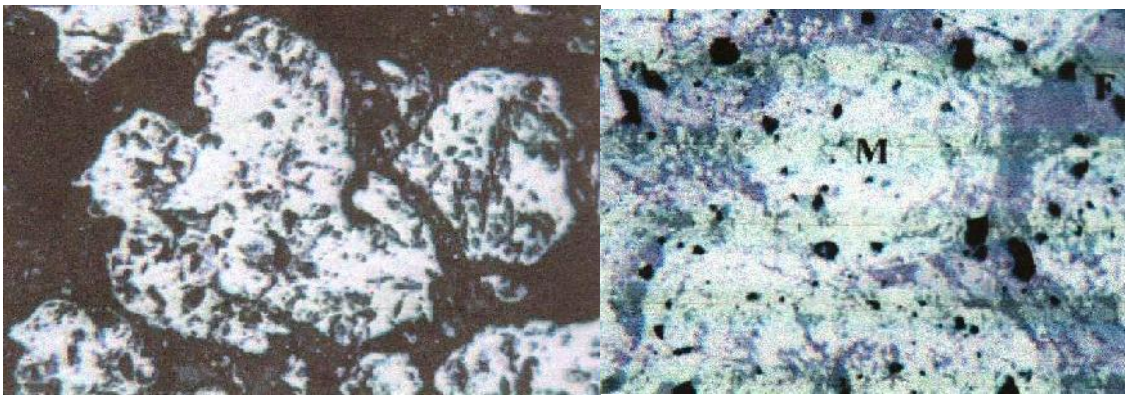

Figure (3- Left): Optical micrograph of a piece of ore embedded in iron slag, mainly magnetite (darker crystals, marked M) and haematite (lighter lamellae, marked H). Black is open porosity and cracks run through this ore, possibly due to an earlier roasting stage.

Figure (3- Right): Optical micrograph of re-crystallised ore, preserving some of the original grain shapes and beginning to form a fayalitic melt phase (darker grey, marked as F). The bulk of the oxides are magnetite (marked as M).

Figure (4- Right): optical micrograph showing blocky fayalite crystals (light grey, marked as F) in a glassy matrix (darker grey), and formation of free iron oxides in the interstitial glass. Black is porosity.

International Journal of Engineering Technology Science and Research
IJETSR
www.ijetsr.com
ISSN 2394 – 3386
Volume 4, Issue 9
September 2017

The electron beam data show that this region is almost exclusively composed of pure iron oxides, with less than 0.5% by weight of other oxides, mostly alumina. The texture of the intergrowth of haematite and magnetite is typical of a geological material heated under oxidising conditions, with the haematite forming as a result of the oxidation. There was no chemical difference between the two phases that the EBAs would reveal, bearing in mind that EBA does not quantify oxygen by analysis.

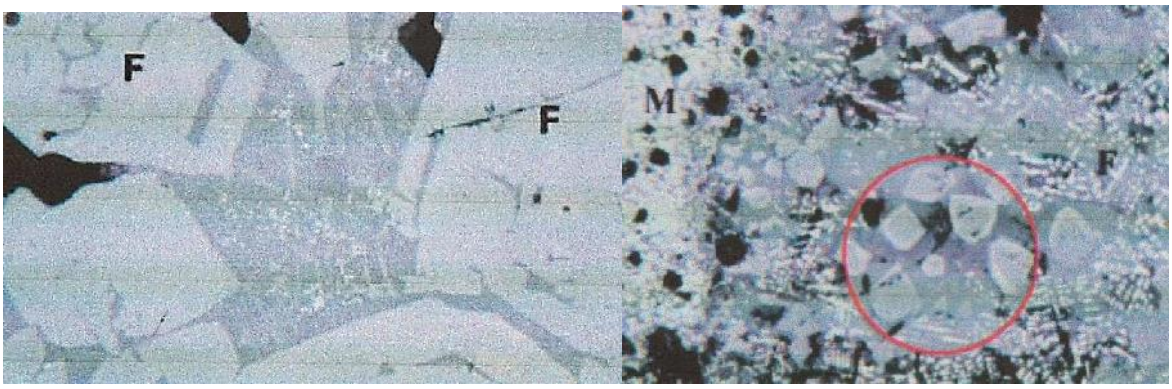

Figure (4- Left): Optical micrograph showing the transition from solid magnetite ore shows fayalitic slag (middle and right, marked as F).

The identification of both iron oxides was confirmed by the Raman spectra of each region (Fig. 4). The lower spectrum of haematite was obtained using an exciting beam of low power ~35 μW, 1% ND filter to prevent degradation of the sample, while the upper one was obtained with a higher beam power ~0.35 mW, 10% ND filter to enhance the signal to noise ratio and to establish whether the material decomposes with increasing beam power.

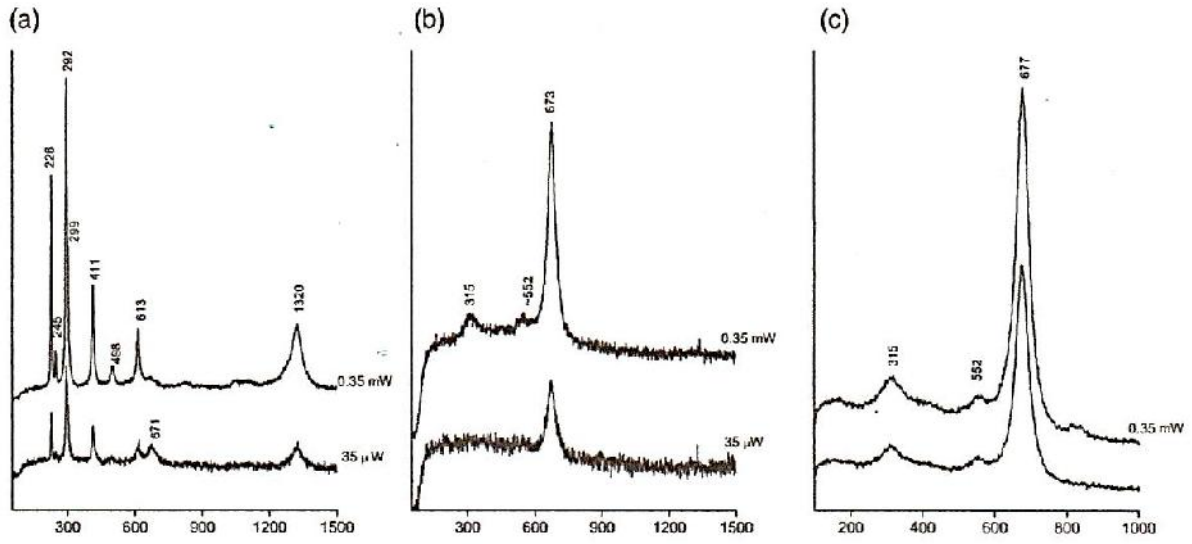

Figure 5(a): Raman Spectra corresponding to haematite (a) and magnetite (b & c)

International Journal of Engineering Technology Science and Research
IJETSR
www.ijetsr.com
ISSN 2394 – 3386
Volume 4, Issue 9
September 2017

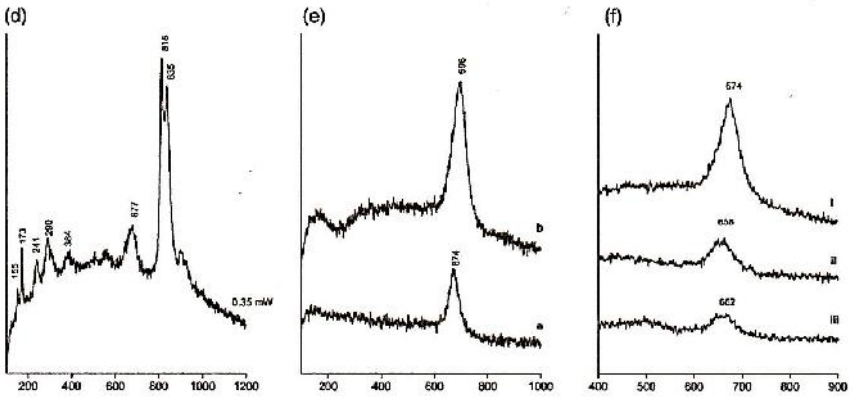

Figure 5(b): Raman Spectra corresponding to fayalite (d) and different compositions with fayalite matrix (e & f).

Sl No	Description	Wavenumber
1	Magnetite	673
2	Magnetite	677
3	Magnetite	674
4	Wustite	662
5	Hercynite	696
6	Magnetite	674
7	Wustite	664

Table 1: Raman Spectra descriptions at various regions of the slag sample

Sl.no.	Name of compound	Concentration (%)
1	CO_2	6.52
2	Na_2O	0.152
3	MgO	0.915
4	Al_2O_3	8.98
5	SiO_2	51.7
6	P_2O_5	2.02
7	SO_3	0.207
8	Cl	0.0891
9	K_2O	3.07
10	CaO	4.38
11	TiO_2	0.348
12	Cr_2O_3	0.0193
13	MnO	0.139
14	Fe_2O_3	21.4
15	SrO	0.0105
16	ZrO_2	0.00933
17	BaO	0.0212

Table 2: Constitutional analysis by FTIR spectra

It was possible to identify the oxidised magnetite and wustite, characterized by a shift to higher wavenumbers of their intense characteristic Raman bands. Further, it also identifies the Al_3^+ substituted magnetite and a

solid solution between magnetite and hercynite ($FeAl_2O_4$). This pilot study aims to develop a model that enables close identification of the redox conditions by analysing the free iron oxides from a variety of smelting processes. It is hoped that this will provide an independent and quantifiable criterion to distinguish smithing slags (more oxidising) from smelting slags (more reducing), and to understand better the actual smelting process that transforms highly oxidised iron ore to fully reduced iron metal.

4. Conclusion:

The following conclusion may be drawn from the above analysis:

a. Haematite (α-Fe_2O_3) and magnetite present in the piece of originalore in the slag.
b. Fayalite (Fe_2SiO_4) present in the intermediate region where the slagbegins to cool, from the reaction between wustite and SiO_2,and mainly crystals of magnetite. These crystals show theRaman band shifted up to 677 cm^{-1}, a shift that maybe explained either by the formation of non-stoichiometricmagnetite or the effect of substitution by Al_3^+, because EBAshows the presence of a small amount of Al_2O_3.
c. In a region that acts as a boundary to the slag itself, there arecrystals of mixed composition in the core and rim. The rimconsists of pure iron oxide, magnetite and the core of a solidsolution of magnetite and hercynite ($FeAl_2O_4$). The distinctionis made by both EBA, which shows a significant percentageof Al_2O_3, and RM, where the main Raman peak is shifted upto 696 cm^{-1}. Fayalite was also identified in this region, alongwith three other types of crystal, namely, puremagnetite, purewustite and an oxidised wustite whose main Raman band isshifted to 662 cm^{-1}.
d. In the last region, where the slag apparently had reactedcompletely, fayalite, magnetite and some wustite wereidentified. A third type of crystal is most likely to be a solidsolution of magnetite and hercynite, with about one-third ofthe theoretical alumina content of pure hercynite.
e. RM proved to be invaluable in the monitoring of fine details of the redox conditions. These analyses are of particular significance for the reconstruction of process parameters in the ancient furnaces.
f. Due to their relatively low operating temperatures (of around 1100 °C), often limited reaction times and slow kinetics, the slag from these furnaces often represents conditions that were prevalent during the main phase of the operation, rather than the more oxidising conditions expected at the end of the process, or during slag tapping. This leads to a gradient from an oxidised skin of haematite and magnetite on the outside of tap slag, in contrast to the much more reduced inner bulk. Being able to monitor this gradient more closely using RM will open up new avenues to reconstruct both process parameters and reaction kinetics in prehistoric iron smelting furnaces.
g. The initial research reported here clearly demonstrates the potential for non-invasive, fast and sensitive phase analysis, revealing information about subtle differences in oxidation state which otherwise are not easily available.

5. Acknowledgement:

The Author would like to thank Dr B S Acharya of IMMT, Bhubaneshwore and Prof R K Gartia of Luminescence Lab at Manipur University for suggesting the problem and their valuable support in making this paper.

6. References

1. Piccardo P, Ienco M G, Balasubramaniam R and Dillman P, Current Science, 87(2004) 650.
2. Dillmann P and Balasubramaniam R, Bulletin of Materials Science, 24 (2001) 317.
3. Balasubramaniam R, NML Tech J, 37 (1995) 123.
4. Godfrey-Smith D I and Casey J L, J ArchaeoSci, 30 (2003) 1037.
5. Rao D V, Sasisekaran B, Satyamurti T, Gartia R K, Badrinarayanan S, Sundararajan S, Rao G S and Rao P C, Sangam: Numismatics and Cultural History (New Era publications, Chennai) 2006, 146-154.

6. Hegde K T M, Ind J HistSci, 16 (1981) 189.
7. Blomgren S and Tholander E, Scamd J Metall, 15 (1986) 151.
8. Prakash B and Igaki K, Ind J HistSci, 19 (1984) 172.
9. Aitken M J, Thermoluminescence Dating (Academic Press, London) 1985, 1-353.
10. Prakash B, Ind J HistSci, 26 (4) (1991) 351.
11. Sheikh R, Nabadwip Singh S, Basanta Singh S and Gartia R K, Sanatan, 19(3) (2009)
12. Gourachandra M, Traditional Iron smelting and forging in Manipur (Peoples Museum Publications, Kakching, Manipur) 1997, 1-37.
13. Vania S. F. Muralha, ThiloRehren and Robin J. H. Clark, Characterization of an iron smelting slag from Zimbabwe by Raman microscopy and electron beam analysis, Journal of Raman Spectroscopy, (Willeyonlinelibrary.com) DOI 10.1002/jrs.2961, June 2011, (2077-2084)
14. Gautier A, QuatSci Rev, 20 (2001) 973.
15. Lars Bøtter-Jensen, Radiat. Meas., 27 (1997) 749
16. Sowmya T and Sankaranarayanan S R, Spectroscopic analysis of slags – preliminary observations (VII International Conference on Molten Slags, Fluxes and Salts, The South African Institute of Mining and Metallurgy, South Africa) January 2004, 693-697.
17. R Sheikh, B S Acharya and R K Gartia, Characterization of iron slag of kakching, Manipur by x-ray and optical spectroscopy, Indian Journal of Pure and Applied Physics, 48(9), 2010, 632-635